J. Fluid Mech. (1978), *vol.* 89, *part* 1, *pp.* 61–78
Printed in Great Britain

Analysis of a cylindrical imploding shock wave

By E. A. MISHKIN AND Y. FUJIMOTO†
Polytechnic Institute of New York, Brooklyn

(Received 5 July 1977 and in revised form 3 March 1978)

The self-similar solution of the gasdynamic equations of a strong cylindrical shock wave moving through an ideal gas, with $\gamma = c_p/c_v$, is considered. These equations are greatly simplified following the transformation of the reduced velocity

$$U_1(\xi) \rightarrow U_1 = \tfrac{1}{2}(\gamma+1)(U+\xi).$$

The requirement of a single maximum pressure, $d_\xi P = 0$, leads to an analytical determination of the self-similarity exponent $\alpha(\gamma)$. For gases with $\gamma < 2+3^{\frac{1}{2}}$ the slight maximum pressure occurs behind the shock front, nearing it as γ increases. For $\gamma \geqslant 2+3^{\frac{1}{2}}$, this maximum ensues right at the shock front and the pressure distribution then decreases monotonically. The postulate of analyticity by Gelfand and Butler is shown to concur with the requirement $d_\xi P = 0$. The saturated density of the gas left in the wake of the shock is computed and $-U$ is shown to be the reduced velocity of sound at $P = P_m$.

1. Introduction

There is an increased interest in the problem of implosion. Among other applications it is viewed as a necessary step in realizing controlled thermonuclear fusion (Nuckolls *et al.* 1972; Clark, Fisher & Mason 1973). As pointed out by Kidder (1974), 'there are two basic ways in which laser induced blow-off pressure can be employed to produce high compression, which represent opposite limits. They are the strong spherically convergent shock [Zeldovich & Raizer 1967] and the shockless or isentropic compression' (Kidder 1974). It is conceivable that a cylindrical configuration may present certain advantages and we consider in the following the general problem of shock waves having a cylindrical symmetry, both exploding or moving away from the axis of symmetry and imploding or converging onto the central axis. At the shock front the entropy is not conserved.

A sudden release of a substantial amount of energy, evenly distributed along the central axis, produces a cylindrical explosion. As time increases, the position $R(t)$ of its shock front increases. The imploding cylindrical shock wave can be thought of as induced by a 'cylindrical piston' converging onto the central axis. We assume the shock wave to move in a perfect gas, with a constant ratio $\gamma = c_p/c_v$, its front reaching the radius $r = R_0$ at time $t = 0$. The explosion occurred t_c seconds earlier. The imploding

† Permanent address: Koyo Seiko Ltd, Japan.

shock wave collapses at the centre t_c seconds later. A strong imploding shock, or a sequence of such shocks, can compress substantially the matter around the axis of symmetry. We assume the gas to present a continuum and neglect its molecular structure, and the dissipative processes associated with it. We consider here a single imploding shock wave up to its collapse time at the axis of symmetry.

With the matter compressible the underlying conservation equations of mass, momentum and energy are the well-known gasdynamic equations written in a cylindrical co-ordinate system (Landau & Lifshitz 1959; Courant & Friedrichs 1957). The system possesses no characteristic length and we consider the self-similar solution of these equations (Taylor 1946). In both cases we attempt an analytical determination of the self-similar exponent, see §§3 and 6. A more detailed analysis of the problem of implosion shock is also presented.

In the case of a strong exploding shock, the energy per unit length released suddenly at the axis of symmetry is conserved. This time independence leads directly to the value, $\alpha = 0{\cdot}5$, of the self-similarity exponent, see §3. Obviously this principle is inapplicable in the case of an imploding shock wave coming from infinity. However, we notice that at the shock front there is a sudden jump in the pressure which continues to increase and reaches a maximum P_m behind the shock front (Zeldovich & Raizer 1967, p. 804 and note). The pressure dies out in the wake of the shock wave. The postulate of a single maximum pressure P_m behind the shock front leads to an analytic determination, in closed form, of the self-similarity coefficient $\lambda(\gamma)$ and $\alpha = 1/(1-\lambda)$, see §6 and figure 1.

The slight maximum in the pressure distribution behind the shock front may escape unobserved in a not very careful numerical solution. At $\gamma = 2+3^{\frac{1}{2}}$, this maximum occurs at the shock front and the pressure distribution function then decreases almost monotonically.

A physically meaningful solution of the conservation equations must be single-valued (Zeldovich & Raizer 1967, p. 801). The shock front presents a discontinuity in the pressure, density and velocity distributions of the gas. Behind the shock front the pressure, density and velocity and their derivatives must be well-behaved functions. The solutions derived in this paper are shown to be both single-valued and non-singular.

Gelfand investigated the nonlinear gasdynamic equations of an imploding shock moving through an ideal gas and showed that there is a whole interval of possible values of the self-similar coefficient λ. He then proposed to choose λ on the basis of analyticity of the resulting solution (Brushlinskii & Kazhdan 1963).† Butler (1954) also investigated the problem of implosion with the aid of a high-speed computer and chose the 'one non-singular solution of a system of nonlinear equations'. Obviously then this postulate of analyticity must coincide with the requirement of a single maximum in the pressure distribution behind the shock front. This is shown in §9.

Section 2 presents the mass, momentum and energy conservation equations and their self-similar solution in the form of products of a time-dependent part $T(t)$

† Brushlinskii & Kazhdan (1963) present a thorough mathematical treatment of the problem of implosion. They report that in 1952 I. M. Gelfand proved that in problems of the type indicated for certain ranges of parameters there exist a whole interval of values of automodel exponents corresponding, generally speaking, to solutions *non*-analytic on the characteristics. He proposed, however, to choose the exponent on the principle of analyticity.

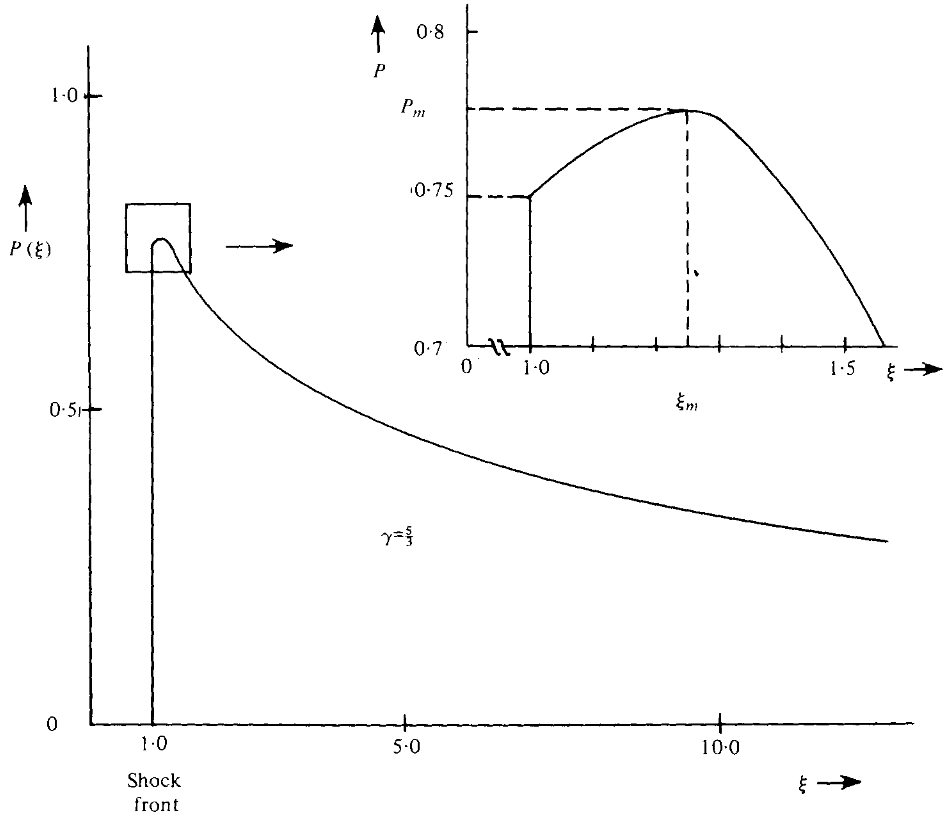

FIGURE 1. The reduced pressure behind a strong cylindrical imploding shock wave in a perfect gas with $\gamma = \frac{5}{3}$.

and a ξ-dependent function $\Xi(\xi)$, $f(r, t) = T(t)\,\Xi(\xi)$. The variable $\xi = r/R(t)$ is non-dimensional, $R(t)$ is the radius of the shock front. A new reduced velocity $U(\xi)$ is introduced that greatly simplifies the expressions of the hydrodynamic derivative and that of the following ordinary differential equations. $U(\xi)$ is shown to be the non-dimensional speed of sound at $P(\xi) = P_m$ (see §7). Following the ξ, $U \to x = d_\xi U$, $y = U/\xi$ transformation presented in §5, the self-similar exponent α is determined analytically in §6, in which the physical admissibility of the proposed solution is also discussed.

2. Basic equations, the self-similar solution

The mass, momentum and energy conservation equations in cylindrical symmetry read (Landau & Lifshitz 1959; Courant & Friedrichs 1957)

$$\left.\begin{aligned} &d_t\rho + \rho\,\partial_r u + \rho\frac{u}{r} = 0; \quad \partial_t \equiv \frac{\partial}{\partial t}; \quad \partial_r \equiv \frac{\partial}{\partial r};\\ &d_t u + \rho^{-1}\partial_r p = 0; \quad d_t \equiv \frac{d}{dt} = \partial_t + u\partial_r;\\ &d_t(p\rho^{-\gamma}) = 0. \end{aligned}\right\} \tag{2.1}$$

p, ρ and u denote the pressure, density, and velocity of the gas assumed ideal with a constant ratio $\gamma = c_p/c_v$.

We consider a shock discontinuity moving through the gas of density ρ_0 and denote by $R(t)$ the position of the shock front and by $\dot{R}(t)$ its velocity. In case of a very strong shock the pressure the shock encounters can be neglected and the pressure, density and gas velocity right behind the shock front are (Courant & Friedrichs 1957; Zeldovich & Raizer 1967)

$$p = \frac{2}{\gamma+1}\rho_0 \dot{R}^2; \quad \rho = \frac{\gamma+1}{\gamma-1}\rho_0; \quad u = \frac{2}{\gamma+1}\dot{R}. \tag{2.2}$$

We measure the position r of any point behind the shock in units of $R(t)$,

$$\xi = \frac{r}{R(t)}, \tag{2.3}$$

and consider the self-similar solution of the conservation equations (2.1),

$$p = \frac{2}{\gamma+1}\rho_0 \dot{R}^2 P(\xi); \quad \rho = \frac{\gamma+1}{\gamma-1}\rho_0 \mathscr{R}(\xi); \quad u = \frac{2}{\gamma+1}\dot{R}U_1(\xi), \tag{2.4}$$

in which the time scales of the pressure, density and gas velocity at any point ξ are exactly the same as at the shock front and the shape of the p, ρ and u distributions is preserved in time. $P(\xi)$, $\mathscr{R}(\xi)$ and $U_1(\xi)$ are the dimensionless reduced pressure, density and velocity, respectively. At the shock front, $\xi = 1$, and

$$P(1) = \mathscr{R}(1) = U_1(1) = 1. \tag{2.5}$$

The derivatives of the product function,

$$f(r,t) = T(t)\,\Xi(\xi), \tag{2.6}$$

with respect to r and t are

$$\begin{aligned} \partial_t f &= \Xi\dot{T} - \frac{\dot{R}}{R}\xi T\Xi'; \\ \partial_r f &= \frac{1}{R}T\Xi'; \\ d_t f &= (\partial_t + u\partial_r)t = \Xi\dot{T} + \left(\frac{2}{\gamma+1}U_1 - \xi\right)\frac{\dot{R}}{R}T\Xi'. \end{aligned} \tag{2.7}$$

The transformation (Fujimoto & Mishkin 1977*a*, *b*)

$$U_1 \to U_1 = \frac{\gamma+1}{2}(U+\xi) \tag{2.8}$$

introduces the new non-dimensional velocity U,

$$u = \dot{R}(U+\xi), \tag{2.9}$$

and simplifies the hydrodynamic derivative (2.7),

$$d_t f = \Xi\dot{T} + U\frac{\dot{R}}{R}T\Xi'. \tag{2.10}$$

At the shock front,

$$U(1) = -\frac{\gamma-1}{\gamma+1}; \tag{2.11}$$

see (2.5) and (2.8). The term $-U(\xi)$ is the reduced speed of sound,

$$-U = [2/(\gamma+1)]\, C(\xi_m),$$

at the point when the pressure $P(\xi)$ is maximum, $d_\xi P = 0$ (see §7). The self-similar solutions (2.4) now reduce the partial differential conservation equations (2.1) to the set of the three ordinary differential equations

$$-\frac{d\mathscr{R}}{\mathscr{R}} = \frac{dU}{U} + \frac{d\xi}{\xi} + 2\frac{d\xi}{U}, \tag{2.12a}$$

$$-2\frac{\gamma-1}{(\gamma+1)^2}\frac{dP}{\mathscr{R}} = U\,dU + \lambda\xi\, d\xi + (1+\lambda)\, U\, d\xi, \tag{2.12b}$$

$$-\frac{dP}{P} = \gamma\left(\frac{dU}{U} + \frac{d\xi}{\xi}\right) + 2(\lambda+\gamma)\frac{d\xi}{U}, \tag{2.12c}$$

where

$$\lambda = \frac{d\ln \dot{R}}{d\ln R}; \tag{2.13}$$

ρ_0 was here assumed constant.

Separation of the variables t and ξ requires $\lambda = \text{const.}$ and hence

$$R(t) = R_0(1 \pm t/t_c)^\alpha; \quad \alpha = \frac{1}{1-\lambda}. \tag{2.14}$$

The time t is measured in units of t_c. At time $t = 0$ the shock front is at R_0. The plus sign corresponds to an exploding shock and the minus sign to an imploding shock wave.

In the implosion case, (2.12a) and (2.12c) are directly integrable, from the shock front at $\xi = 1$ to some arbitrary point ξ behind it, but for the last term. We formally then introduce

$$\sigma(\xi) = \exp\left[-\int_1^\xi \frac{d\xi'}{U(\xi')}\right]; \quad \sigma(1) = 1; \quad d_\xi\sigma(\xi) = -\frac{\sigma(\xi)}{U(\xi)}; \tag{2.15}$$

$$\sigma(\infty) = \exp\left[-\int_1^\infty \frac{d\xi}{U(\xi)}\right].$$

It is shown below that

$$\frac{\gamma-1}{\gamma+1}\lim_{\xi\to\infty}\left[\frac{\sigma(\xi)}{\xi}\right]^2$$

defines the maximum compression ratio $\rho(\infty)/\rho(0)$ that can be achieved by means of a single strong cylindrical imploding shock; see (8.2).

In the following the exponent α of the self-similar solution is to be found analytically for both kinds of shock wave.

3. Cylindrical exploding shock wave

We assume a finite energy E per unit length, released suddenly along the cylindrical axis at time $t = -t_c$. A strong shock is created whose front t_c seconds later reaches R_0. When E is large and the shock front is not too far away from the axis of symmetry, the pressure the shock encounters can be neglected. The energy E transmitted to the gas behind the cylindrical shock is then conserved or time independent,

$$E = \int_0^R \left(\frac{p}{\gamma-1} + \tfrac{1}{2}\rho u^2\right) 2\pi r\, dr = \frac{4\pi\alpha^2}{(\gamma^2-1)\,t_c^2}\rho_0 R_0^4 \left(1+\frac{t}{t_c}\right)^{4\alpha-2} \int_0^1 (P+\mathscr{R}U_1^2)\,\xi\, d\xi$$
$$= \text{const.} \tag{3.1}$$

See (2.3), (2.4) and (2.14), whence $\alpha = 0{\cdot}5.$ (3.2)

When the exploding shock is spherically symmetric the self-similarity exponent $\alpha = 0{\cdot}4$. (See Stanyukevich 1960.)

4. Imploding shock waves

The centre-axis-bound imploding shock wave is produced by some kind of converging 'cylindrical piston'. The determination of the value of the self-similar exponent α, (2.14),

$$R(t) = R_0\left(1-\frac{t}{t_c}\right)^{\alpha},$$

cannot follow the simple energy conservation principle applied in the previous section, or some dimensional considerations. It is based here on the following pressure considerations. For the sake of simplicity we consider strong shocks only where the initial pressure of the gas and its internal energy through which the shock wave moves can be neglected. At the shock front the imploding wave causes a sudden rise in the pressure which at first increases, for small values of ξ, and then decreases until it vanishes at the tail of the shock at $\xi = \infty$ (Zeldovich & Raizer 1967, p. 804 and note). The pressure then reaches a maximum, or

$$d_\xi P = 0, \tag{4.1}$$

at some value of ξ behind the shock front (Fujimoto & Mishkin 1977*a*, *b*). This maximum $P_m(\xi)$ occurs behind the shock front for all gases for which $\gamma < 2+3^{\frac{1}{2}}$. For $\gamma = 2+3^{\frac{1}{2}}$, P_m occurs right at the shock front; see (6.9).

The shock front represents a discontinuity in all the functions representing pressure, density, or velocity of the gas. Behind it all these functions, and their derivatives, are well-behaved functions. Gelfand proposed then to choose the self-similarity solution on the principle of analyticity (Brushlinskii & Kazhdan 1963; Butler 1954).

In order for the solution of the gasdynamic equations to be physically meaningful, it must be single-valued (Zeldovich & Raizer 1967, p. 801). The dimensionless density and pressure follow a direct integration of (2.12*a*) and (2.12*c*) from the shock front at $\xi = 1$ to some arbitrary point ξ behind it,

$$\mathscr{R}(\xi) = -\frac{\gamma-1}{\gamma+1}\frac{\sigma^2(\xi)}{\xi U(\xi)}; \tag{4.2}$$

$$P(\xi) = \left[\frac{1-\gamma}{1+\gamma}\frac{1}{\xi U(\xi)}\right]^{\gamma} \sigma^{2(\lambda+\gamma)};$$

see (2.15).

It follows from (2.12*b*, *c*), (2.5) and (2.11) that at the shock front

$$d_\xi U(1) = -\frac{6\lambda(\gamma+1)+\gamma^2+6\gamma+1}{(\gamma+1)^2}. \tag{4.3}$$

Since the non-dimensional velocity U_1 of the gas is a monotonically decreasing function of ξ, the slope of U_1 at the shock front is negative,

$$d_\xi U(1) < -1; \tag{4.4}$$

see (2.8). In the wake of the shock, at $\xi = \infty$, the gas is back at rest and the non-dimensional velocity vanishes,

$$U_1(\infty) = 0, \tag{4.5}$$

leading to

$$U(\xi \to \infty) = -\xi; \quad d_\xi U(\infty) = -1. \tag{4.6}$$

In the following computations the slope of the non-dimensional pressure curve versus ξ proves to be of prime importance. Its value at the shock front is

$$d_\xi P(1) = -2\frac{2\gamma-1}{\gamma-1}(\lambda-\lambda_0); \tag{4.7}$$

$$\lambda_0 = -\frac{\gamma(\gamma-1)}{(\gamma+1)(2\gamma-1)},$$

see (2.5), (2.11), (2.12) and (4.3). It is positive, i.e. the pressure has a maximum behind the shock front, when

$$d_\xi P(1) > 0, \quad \text{when} \quad \lambda < \lambda_0. \tag{4.8}$$

The velocity U_1, pressure P, and density $\mathscr{R}$ are all functions of U. The differential equation of U follows from (2.12*b*, *c*),

$$\sigma^{2(\lambda+\gamma-1)} = -\frac{U d_\xi U + (1+\lambda)U + \lambda\xi}{\gamma(\xi d_\xi U + U) + 2(\lambda+\gamma)\xi}\frac{(\gamma+1)^{\gamma+1}}{2}\left[\frac{\xi U}{1-\gamma}\right]^\gamma; \tag{4.9}$$

see (2.15) and (4.2). Its logarithmic derivative reads

$$2\frac{\lambda+\gamma-1}{U} = \frac{2\gamma d_\xi U + \gamma\xi d_\xi^2 U + 2(\lambda+\gamma)}{\gamma\xi d_\xi U + 2(\lambda+\gamma)\xi + \gamma U} - \gamma\frac{U+\xi d_\xi U}{\xi U} - \frac{(d_\xi U)^2 + U d_\xi^2 U + (\lambda+1)d_\xi U + \lambda}{U d_\xi U + (\lambda+1)U + \lambda\xi}. \tag{4.10}$$

5. The x, y plane

The differential equation of U is a difficult nonlinear one and it is instructive to consider it in the U/ξ, $dU/d\xi$ plane. We then introduce the transformation $\xi, U \to x, y$, where x and y denote the ratios

$$x = d_\xi U; \quad y = \frac{U}{\xi}; \quad \frac{x}{y} = \frac{d\ln U}{d\ln\xi}, \tag{5.1}$$

which reduce (4.10) to a first-order differential equation and cast it in a form amenable to an analytical determination of the self-similarity exponent α presented in the next section. It also shows that the reduced pressure $P(\xi)$ reaches a maximum $P_m(\xi)$ behind the shock front and determines its value and position (x_m, y_m) in the new x, y plane. Similarly, the density of the gas in the wake of the shock is shown to saturate at the value found in §8.

The derivative relationships

$$d_\xi x = d_\xi^2 U; \quad d_\xi y = \frac{x-y}{\xi}; \quad \xi d_\xi^2 U = \frac{x-y}{d_x y} \tag{5.2}$$

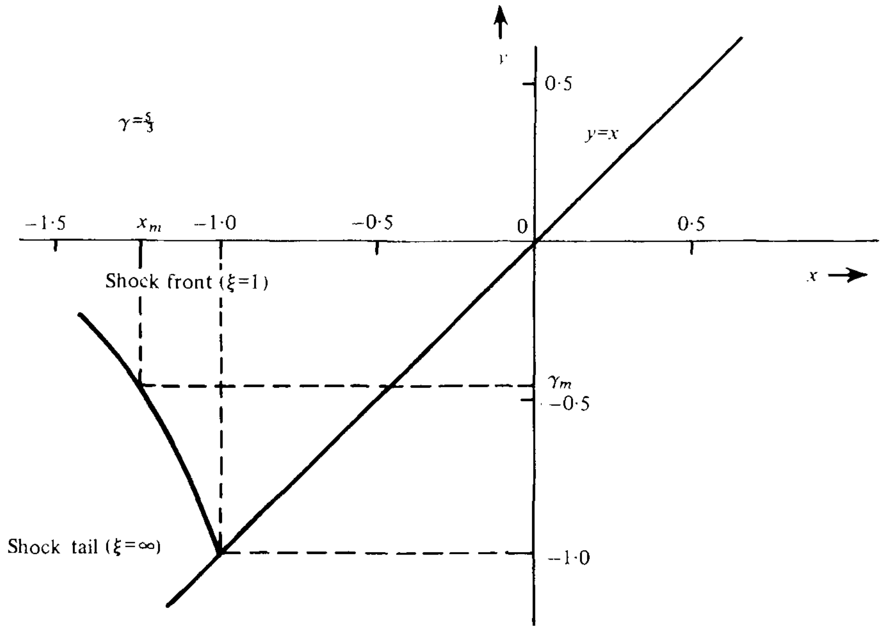

FIGURE 2. Motion of the strong cylindrical imploding shock in a perfect gas with $\gamma = \frac{5}{3}$ in the x, y plane. x_m, y_m denote the point at which the pressure is at its maximum.

follow directly from the definition (5.1). Substitution of these relationships into (4.10) results in the derivative form of the curve in the x, y plane,

$$d_x y = \frac{y(y-x)\left[\gamma y^2 + (\gamma + 2\lambda - \gamma\lambda)\, y - \gamma\lambda\right]}{G(x, y; \lambda)}, \tag{5.3}$$

where
$$\begin{aligned} G(x, y; \lambda) = {} & [\gamma(x+y+2) + 2(\lambda-1)]\,[\gamma(x+y+2) + 2\lambda]\,[y(x+\lambda+1)+\lambda] \\ & - 2y[\gamma(x+1)+\lambda]\,[y(x+\lambda+1)+\lambda] \\ & + y[x^2 + (1+\lambda)\,x + \lambda]\,[\gamma(x+y+2)+2\lambda]. \end{aligned} \tag{5.4}$$

$G(x, y; \lambda) = 0$, at the point (x_m, y_m) discussed below, on the curve (5.3); see figure 2.

At the front of the shock, $\xi = 1$ and $y(1) = U(1)$; $x(1) = d_\xi U(1)$ are given by (2.11) and (4.3), respectively,

$$x(1) = -\frac{6\lambda(\gamma+1) + \gamma^2 + 6\gamma + 1}{(\gamma+1)^2} < -1; \quad y(1) = -\frac{\gamma-1}{\gamma+1} < 0. \tag{5.5}$$

At the other end of the (5.3) curve, in the wake of the shock

$$x(\infty) = y(\infty) = -1; \tag{5.6}$$

see (4.6).

6. Analytical determination of the self-similarity coefficient λ

The pressure vanishes in the wake of the shock wave,

$$\lim_{\xi \to \infty} P(\xi) = 0. \tag{6.1}$$

When the pressure rises at the shock front,

$$d_\xi P(\xi)|_{\xi=1} > 0, \tag{6.2}$$

$P(\xi)$ must have a maximum at some value, $1 < \xi < \infty$, behind the shock front. Its derivative at this point $d_\xi P(\xi) = 0$. Following the $\xi, U \to x, y$ transformation (5.1), (2.12*b*) and (2.12*c*) then take the form

$$\begin{aligned} xy+(\lambda+1)\,y+\lambda &= 0; \\ \gamma(x+y)+2(\lambda+\gamma) &= 0, \end{aligned} \tag{6.3}$$

or

$$\gamma y^2+y(\gamma+2\lambda-\gamma\lambda)-\gamma\lambda = 0. \tag{6.4}$$

The reduced pressure has a single maximum $P_m(\xi_m)$ when the discriminant Δ of the last quadratic equation is zero† (see also appendix),

$$\lambda = \lambda_m = -\frac{\gamma}{(\gamma^{\frac{1}{2}}+2^{\frac{1}{2}})^2}. \tag{6.5}$$

The maximum pressure P_m occurs at the point (x_m, y_m) on the (5.3) curve,

$$\begin{aligned} y_m &= -(-\lambda_m)^{\frac{1}{2}} = -\frac{\gamma^{\frac{1}{2}}}{\gamma^{\frac{1}{2}}+2^{\frac{1}{2}}}; \\ x_m &= -\left[1+\frac{(2\gamma)^{\frac{1}{2}}}{(\gamma^{\frac{1}{2}}+2^{\frac{1}{2}})^2}\right]. \end{aligned} \tag{6.6}$$

As the value of y varies from $y(1)$ to $y(\infty) = -1$ (see (5.5) and (5.6)), it equals y_m at some ξ_m. At this point, with $\lambda = \lambda_m$, the value of x is x_m given by (6.6); see figure 2.

The value of the maximum pressure $P_m(\xi)$ can be obtained with the aid of (4.2),

$$P_m(\xi_m) = \left[\frac{1-\gamma}{1+\gamma}\xi_m^{-2}y_m^{-1}\right]^\gamma \sigma^{2(\lambda+\gamma)}(\xi_m), \tag{6.7}$$

where

$$\sigma(\xi_m) = \exp\left[-\int_1^{\xi_m}\frac{d\xi}{U}\right] = \exp\left[-\int_{y(1)}^{y_m}\frac{dy}{y(x-y)}\right], \tag{6.8}$$

see (2.15) and (5.2).

We note that the derivative form $d_x y$ of the curve (5.3) is non-singular for although its denominator $G(x, y; \lambda_m)$ vanishes at (x_m, y_m) when the pressure is maximum, $d_\xi P = 0$, and at the tail of the shock, when $x(\infty) = y(\infty) = -1$ (see (5.4) and (6.3)), the numerator of (5.3) also vanishes at these two points; see (5.3) and (6.4).

We shall consider now in greater detail the functional dependence $\lambda(\gamma)$. We note that two ranges of γ are to be distinguished: (*a*) $1 < \gamma < 2+3^{\frac{1}{2}}$ and (*b*) the physically less important domain $2+3^{\frac{1}{2}} < \gamma$.

(*a*) $1 < \gamma < 2+3^{\frac{1}{2}}$

In this domain, as shown before, the pressure reaches the value P_m at some point behind the shock, the discriminant of the quadratic (6.4) is zero and $\lambda(\gamma) = \lambda_m$ is given by (6.5). Tables 1 and 2 show the values of λ_m and α_m given in closed form by

† The discriminant of the quadratic equation (6.4) also equals zero when

$$\lambda = \lambda_m = -\gamma/(\gamma^{\frac{1}{2}}-2^{\frac{1}{2}})^2.$$

This value of λ must be rejected, for it violates the inequality (5.5).

γ	1·1	11/9	9/7	7/5	5/3	3	$2+3^{\frac{1}{2}}$
$\lambda_m = -\dfrac{\gamma}{(\gamma^{\frac{1}{2}}+2^{\frac{1}{2}})^2}$	−0·181	−0·193	−0·198	−0·207	−0·228	−0·303	−0·333
$\alpha_m = \dfrac{1}{1-\lambda_m}$	0·847	0·838	0·835	0·828	0·814	0·767	0·750
α_m derived numerically	0·885§	0·858§	0·849§	0·835*†§ 0·834‡	0·815*†§	0·775§ 0·810*	0·771§

TABLE 1. The self-similarity coefficients λ_m and the self-similar exponents α_m for various values of $\gamma \leqslant 2+3^{\frac{1}{2}}$. The numerically computed values of α_m are those given by:

* Guderley (1942).
† Butler (1954).
‡ Stanyukevich (1960).
§ Lazarus & Richtmyer (1977); the values of α_m for $\gamma = \frac{11}{9}, \frac{9}{7}$ and $2+3^{\frac{1}{2}}$ are extrapolated.

γ	4	5	6	10	∞
$\lambda_0 = \dfrac{-\gamma(\gamma-1)}{(2\gamma-1)(\gamma+1)}$	−0·343	−0·370	−0·390	−0·431	−0·5
$\alpha_0 = \dfrac{1}{1-\lambda_0}$	0·745	0·730	0·719	0·699	0·667
Numerically computed values of α_0	0·763	0·756	0·751	0·741	0·500* 0·727

TABLE 2. The self-similarity parameter λ_0 and self-similarity coefficient α_0 for various values of $\gamma > 2+3^{\frac{1}{2}}$. The numerically computed values of α_0 are taken from Lazarus & Richtmyer (1977).

* Value given by Stanyukevich (1960).

(2.14) and (6.5), and also those derived with the aid of a computer (see Guderley 1942; Butler 1954; Stanyukevich 1960; Lazarus & Richtmyer 1977). The curves of $\lambda_m(\gamma)$ and $\lambda_0(\gamma)$ [see (4.7)] are shown in figure 3.

Equations (5.5) and (6.6) show that, for $\gamma = 2+3^{\frac{1}{2}}$, the pressure has its maximum right at the shock front,

$$x_m = x(1); \quad y_m = y(1), \quad \text{at} \quad \gamma = 2+3^{\frac{1}{2}}. \tag{6.9}$$

Also at this point, $$\lambda_m = \lambda_0; \quad d_\xi P(1) = 0; \quad \text{for} \quad \gamma = 2+3^{\frac{1}{2}}. \tag{6.10}$$

The slope of the pressure curve at the shock front is then zero; see (4.7). The ratio of the y_m co-ordinate of the maximum pressure to $y(1)$ at the shock front, as a function of γ, is shown in figure 4.

Let us examine the other regions of the λ, γ plane, shown in figure 3. In the region A, $\lambda < \lambda_m$, the discriminant $\Delta < 0$, and the left-hand side of (6.4) never vanishes. In the B region the discriminant of the quadratic (6.4) is positive. The double zero of (6.4) at (x_m, y_m) (see figure 2) splits; there are now two solutions of (6.4), y_1, y_2, at which $d_\xi P = 0$, both behind the shock front. The pressure distribution $P(\xi)$ is as shown in figure 5(*a*); it has a minimum and a maximum. It is seen that at the shock front the slope of the pressure distribution is negative, $d_\xi P(1) < 0$, contrary to that postulated by (4.7), which must be positive for $\lambda_m < \lambda < \lambda_0$.

In the C region, $\lambda > \lambda_0$ and as can be easily shown the two zeros y_1, y_2 of the

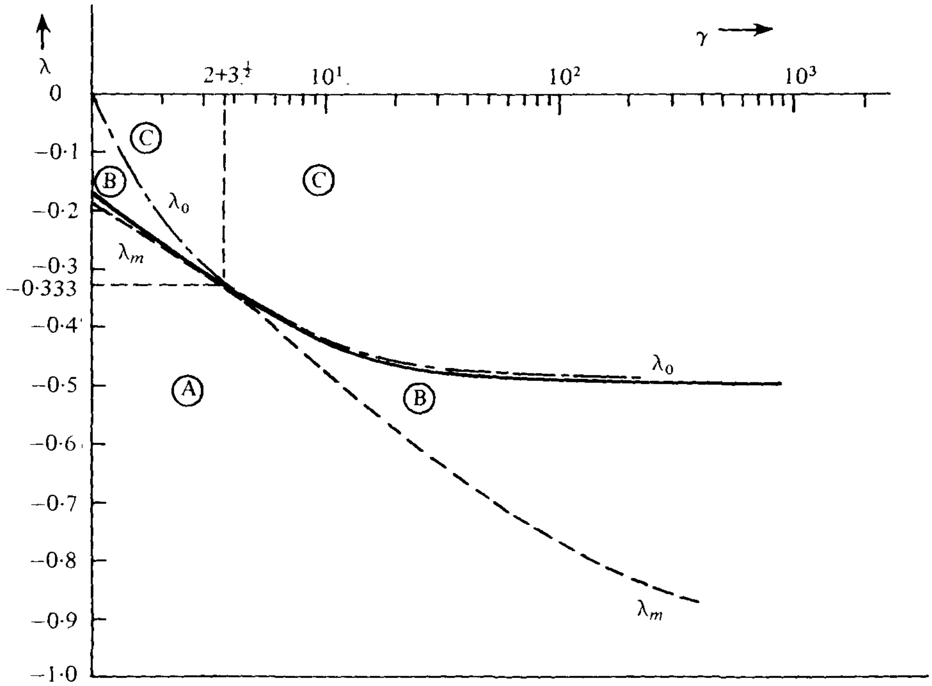

FIGURE 3. The self-similarity coefficient λ, $\alpha = 1/(1-\lambda)$, as a function of γ. ---, $\lambda_m = -\gamma(\gamma^{\frac{1}{2}}+2^{\frac{1}{2}})^2$; —·—, $\lambda_0 = -\gamma(\gamma-1)/(\gamma+1)(2\gamma-1)$; ——, the self-similar solution.

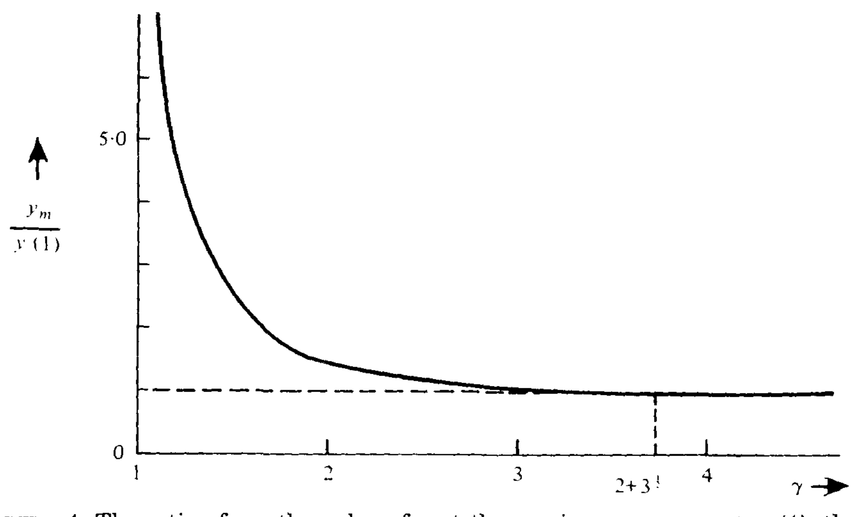

FIGURE 4. The ratio of y_m, the value of y at the maximum pressure, to $y(1)$, the value of y at the shock front, as a function of γ. *For* $\gamma > 2+3^{\frac{1}{2}}$, y_m *occurs at the shock front.*

quadratic (6.4) now occur, one ahead of the shock front at $\xi < 1$, and the other behind it at $\xi > 1$; see figure 5(*b*). The slope $d_\xi P(1)$ of the shock front is now positive, again contradicting (4.7).

$\lambda = \lambda_m$ [see (6.5)] then is the only physically admissible solution for $1 < \gamma < 2+3^{\frac{1}{2}}$. This is shown again in the next section, where it is evident that $-U$ is the speed of sound, at $P = P_m$, $U(\xi_m) = [2/(\gamma+1)]\,C(\xi_m)$.

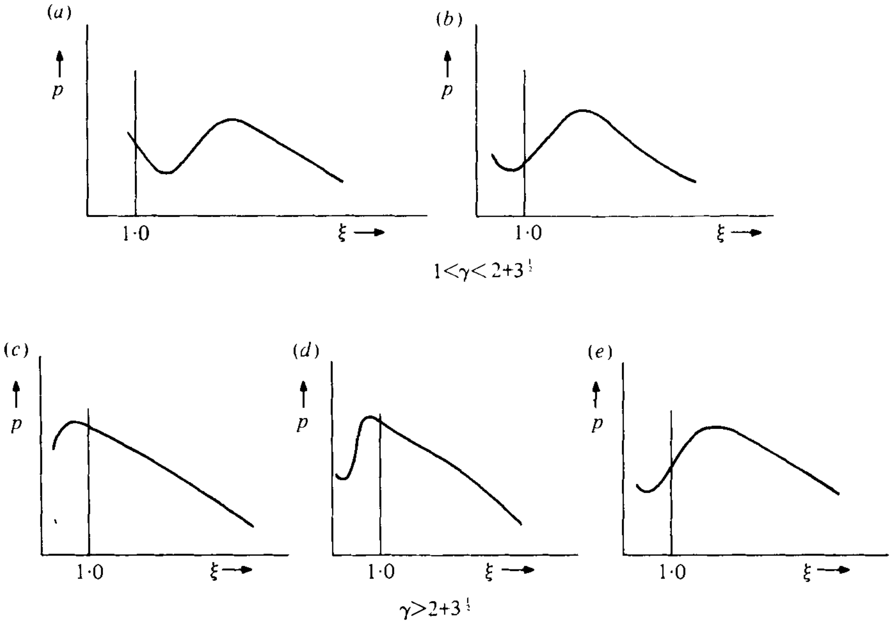

FIGURE 5. Considerations of the self-similarity coefficient λ occurring in the various domains of the λ, γ plane shown in figure 3 and the slope of the pressure curve at the shock front $d_\xi P(1)$. (*a*) Region B, $\lambda_m < \lambda < \lambda_0$. (*b*) Region C, $\lambda_0 < \lambda < 0$. (*c*) $\lambda = \lambda_m$. (*d*) Region B, $\lambda_m < \lambda < \lambda_0$. (*e*) Region C, $\lambda_m < \lambda < \lambda_0$.

(*b*) $\gamma > 2+3^{\frac{1}{2}}$

In this domain, (4.7),
$$\lambda = \lambda_0 = -\frac{\gamma(\gamma-1)}{(\gamma+1)(2\gamma-1)}.$$

The discriminant of the quadratic (6.4) is now positive and the pressure reaches a maximum right at the shock front, after which it decreases monotonically (Zeldovich & Raizer 1967).

It was shown that, at $\lambda = \lambda_m$, the pressure distribution has one maximum only which at $\gamma = 2+3^{\frac{1}{2}}$ occurs right at the shock front; see (6.9). At larger values of γ this maximum occurs in the non-physical region, ahead of the shock wave, where $0 < \xi < 1$; see figure 5(*c*). In the B region, now where $\lambda_m < \lambda < \lambda_0$, the discriminant of the quadratic (6.4) is positive and $d_\xi P = 0$ at two points, both of them still ahead of the shock front (see figure 5(*d*)). In the C region, $\lambda_0 < \lambda < 0$, and the two points at which $d_\xi P = 0$ now are one ahead of the shock front and the other behind it (see figure 5(*e*)). It is easily seen that in all these three cases the slope of the pressure distribution at the shock front $d_\xi P(1)$ is of a sign that contradicts (4.7), leaving $\lambda = \lambda_0$ as the only physically admissible solution for $d_\xi P(1) = 0$; see (4.7).

$$\lambda = \begin{cases} \lambda_m = \dfrac{-\gamma}{(\gamma^{\frac{1}{2}}+2^{\frac{1}{2}})^2} & \text{for} \quad 1 < \gamma < 2+3^{\frac{1}{2}}; \\[2ex] \lambda_0 = \dfrac{-\gamma(\gamma-1)}{(\gamma+1)(2\gamma-1)} & \text{for} \quad 2+3^{\frac{1}{2}} < \gamma; \end{cases} \tag{6.11}$$

see figure 3.

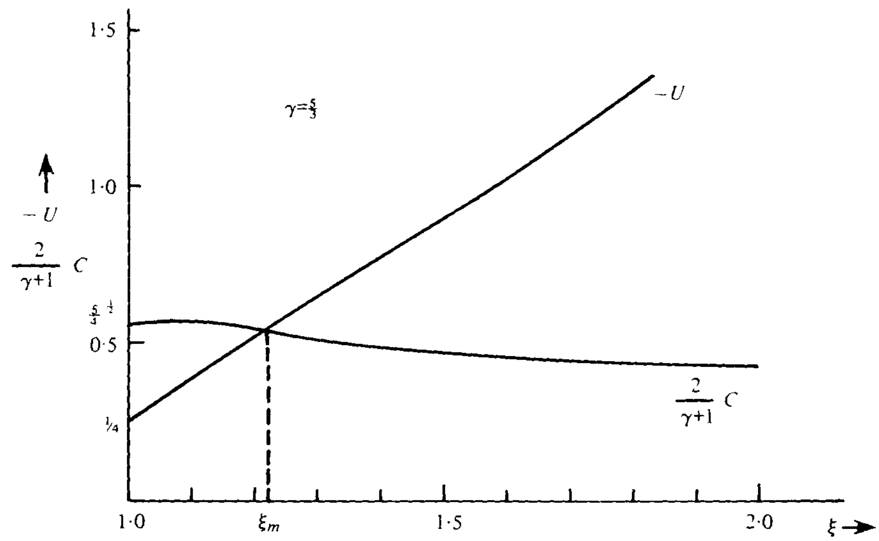

FIGURE 6. The curves of the reduced velocity U and the reduced speed of sound $[2/(\gamma+1)]\,C$ behind the shock front.

Table 2 shows the values of λ_0 and $\alpha_0 = 1/(1-\lambda_0)$, computed with the aid of (4.7), and compares them with the hitherto available numerical values of α_0.

7. The reduced velocity U

U was formally introduced in § 2 in order to simplify the expression for the hydrodynamic derivative (2.10) and in turn the ordinary differential equations (2.12). We shall now show that $-U$ is the speed of sound, but for a γ-dependent constant, at the point where the pressure is maximum behind the shock front,

$$-U(\xi_m) = \frac{2}{\gamma+1}C(\xi_m); \quad 1 < \gamma < 2+3^{\frac{1}{2}}, \tag{7.1}$$

see figure 6 and (7.6).

Equations (2.12*b*) and (2.12*c*) read

$$xy+(1+\lambda)y+\lambda = -2\frac{\gamma-1}{(\gamma+1)^2}\frac{d_\xi P}{\xi\mathscr{R}}; \tag{7.2}$$

$$\gamma(x+y)+2(\gamma+\lambda) = -U\frac{d_\xi P}{P}.$$

We used here the transformation (5.1). Eliminating x we obtain

$$\gamma y^2+(2\lambda+\gamma-\gamma\lambda)y-\lambda\gamma = -\left[\frac{4}{(\gamma+1)^2}C^2-U^2\right]\frac{d_\xi P}{\xi P}, \tag{7.3}$$

where the reduced speed of sound of the ideal gas $C(\xi)$ is $\lambda(\gamma)$ dependent,

$$c^2 = \gamma\frac{p}{\rho} = \frac{4}{(\gamma+1)^2}\dot{R}^2C^2; \quad C^2(\xi) = \gamma\frac{\gamma-1}{2}\frac{P(\xi)}{\mathscr{R}(\xi)}; \tag{7.4}$$

see (2.4).

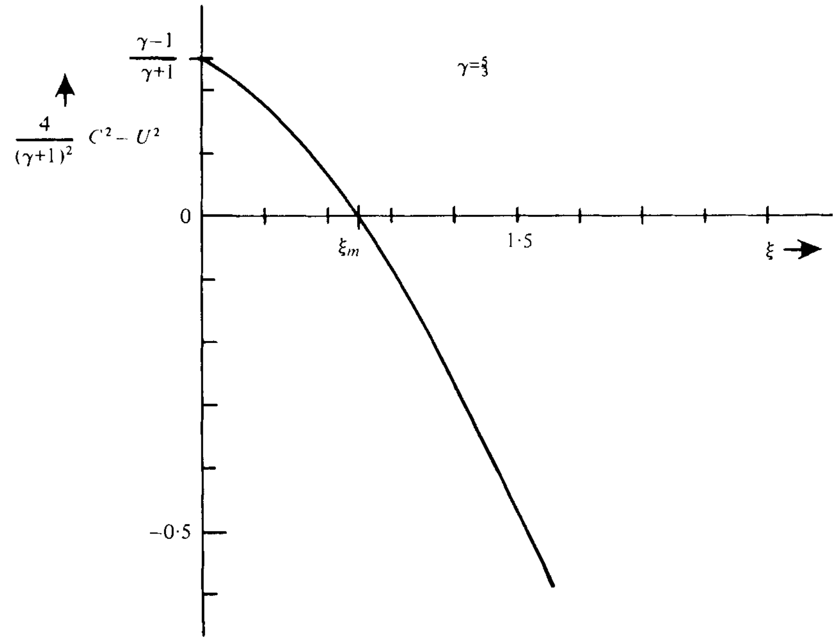

FIGURE 7. The $[4/(\gamma+1)^2]\,C^2-U^2$ versus ξ curve.

In the interval $1<\gamma<2+3^{\frac{1}{2}}$, when $\lambda=\lambda_m$, (7.3) takes the form

$$\gamma(y-y_m)^2=-\left[\frac{4}{(\gamma+1)^2}C^2-U^2\right]\frac{d_\xi P}{\xi P}. \tag{7.5}$$

See (6.6). At (x_m, y_m) the pressure is at its maximum and $d_\xi P=0$. The left-hand side of the last equation is an even function of y around y_m, where it vanishes. On the right-hand side of this equation $d_\xi P$ is an odd function of y around y_m, where it also vanishes; see figures 1 and 2. It follows that

$$\frac{4}{(\gamma+1)^2}C^2-U^2=0 \quad \text{at} \quad d_\xi P=0. \tag{7.6}$$

Around y_m, $[4/(\gamma+1)^2]\,C^2-U^2$ is an odd function of y, see figure 7.

At the shock front, $C^2=\frac{1}{2}\gamma(\gamma-1)$, and

$$\frac{4}{(\gamma+1)^2}C^2(1)-U^2(1)=\frac{\gamma-1}{\gamma+1}; \tag{7.7}$$

see (2.5), (2.11) and (7.4). At very large values of ξ,

$$\frac{4}{(\gamma+1)^2}C^2-U^2\to-\xi^2 \quad \text{for} \quad \xi\gg 1; \tag{7.8}$$

see (4.6). The $[4/(\gamma+1)^2]\,C^2-U^2$ curve is shown in figure 7. It passes the ξ axis at ξ_m, where $P=P_m$. As γ increases from 1 to $2+3^{\frac{1}{2}}$, ξ_m tends towards the shock front at $\xi=1$. Figure 8 shows ξ_m as a function of γ. Even at small values of γ, ξ_m is very close to 1 and the pressure reaches a maximum close to the shock front.

Equation (7.6) proves that the discriminant of the quadratic on the left-hand side of (6.4) or (7.3) cannot be positive in the domain, $1<\gamma<2+3^{\frac{1}{2}}$, or that the solution

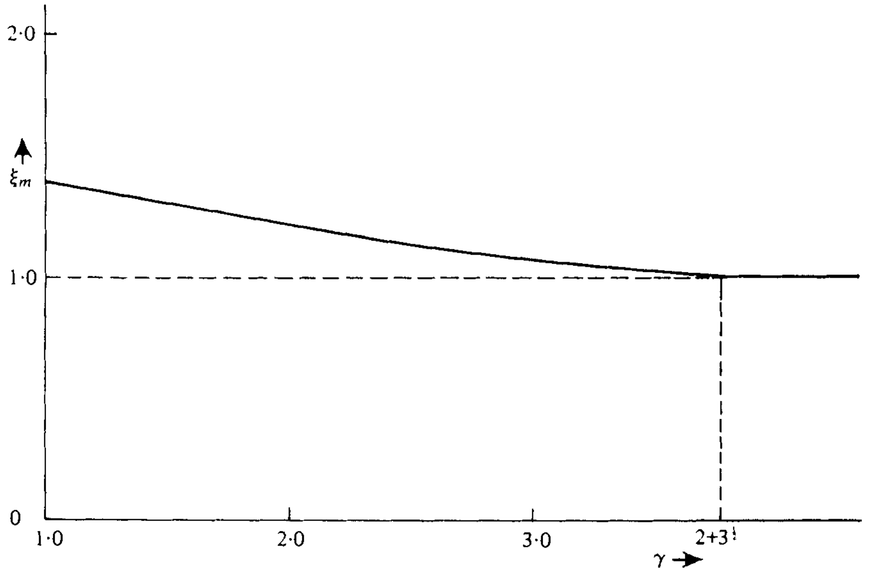

FIGURE 8. The self-similar variable ξ_m, at the point where the pressure reaches maximum, as a function of γ.

$\lambda(\gamma)$ cannot be found in the domains Ⓑ or Ⓒ of figure 3. When the discriminant is positive, there are two values y_1, y_2 at which the left-hand side of (7.3) vanishes,

$$\gamma(y-y_1)(y-y_2) = -\left[\frac{4}{(\gamma+1)^2}C^2 - U^2\right]\frac{d_\xi P}{\xi P}, \tag{7.9}$$

at (x_1, y_1) and (x_2, y_2) [x_1, x_2 are obtained by inserting the values of y_1, y_2 into (6.3)]. When passing through y_1 or y_2 the left-hand side of the last equation changes sign and $[4/(\gamma+1)^2]/C^2 - U^2$ now cannot vanish at $d_\xi P = 0$. The function $d_\xi P$ now is odd around y_1 and y_2. The right-hand side of (7.9) then vanishes at three values of y while the left-hand side is zero only at two. In the Ⓒ domain $\lambda_0 < \lambda$ (see figure 5 (*b*)), the left-hand side of (7.9) vanishes at one point only behind the shock front, while the right-hand side of (7.9) would have to vanish at two.

A similar argument made for gases with $\gamma > 2 + 3^{\frac{1}{2}}$ shows that now the only physically admissible solution is $\lambda = \lambda_0$ [see (4.7)] in agreement with the slope of the pressure curve consideration of the previous section.

8. The density of the gas in the wake of a strong imploding cylindrical shock

A strong imploding cylindrical shock moving through a gas of density ρ_0 compresses the gas behind it to the density $\rho(\infty, t)$, which is finite and independent of the strength of the shock. It depends upon the ratio γ only. The final reduced density,

$$\frac{\rho(\infty, t)}{\rho_0} = \frac{\gamma+1}{\gamma-1}\mathscr{R} \quad (\xi = \infty) \tag{8.1}$$

(see (2.4)), follows directly from (4.2),

$$\mathscr{R}(\xi) = -\frac{\gamma-1}{\gamma+1}\xi^{-1}U^{-1}(\xi)\,\sigma^2(\xi).$$

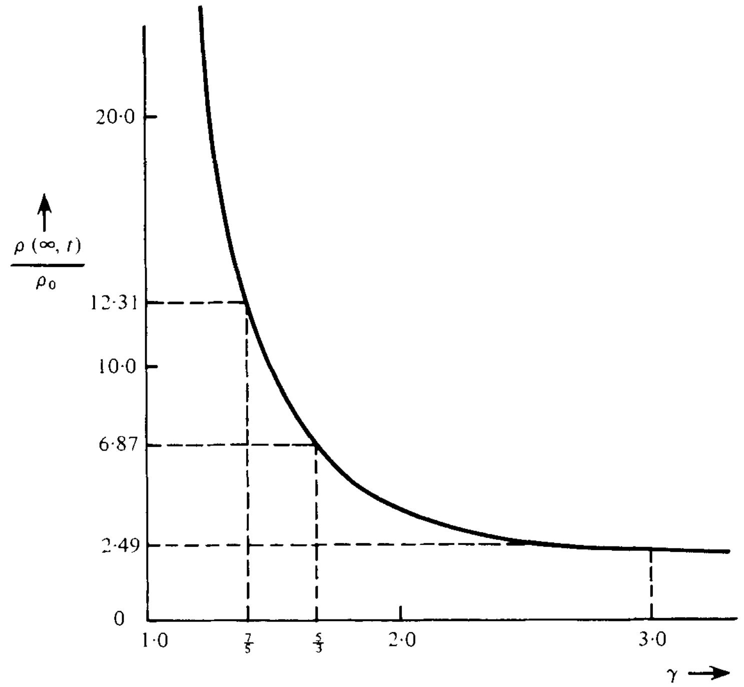

FIGURE 9. The saturated density of the ideal gas under the impact of a single strong imploding shock.

γ	$\frac{11}{9}$	$\frac{7}{5}$	$\frac{5}{3}$	3	∞
$\dfrac{\rho(\infty,t)}{\rho_0} = \dfrac{\gamma+1}{\gamma-1}\mathrm{P}(\infty)$	28·91	12·31	6·87	2·49	1·0

TABLE 3. The final density of an ideal gas in the wake of a strong imploding cylindrical shock.

At the tail of the shock, when $\xi \to \infty$, the gas is again at rest and, (4.6),

$$\lim_{\xi\to\infty} U(\xi) = -\xi.$$

The reduced density of the gas left in the wake of the cylindrical shock is

$$\frac{\rho(\infty,t)}{\rho_0} = \lim_{\xi\to\infty}\left[\frac{\sigma(\xi)}{\xi}\right]^2 = \lim_{\xi\to\infty}\left[\frac{1}{\xi}\exp\left\{-\int_1^{\xi}\frac{d\xi'}{U(\xi')}\right\}\right]^2, \tag{8.2}$$

see (2.15).

Figure 9 and table 3 show the saturated gas density, left in the wake of a single strong shock with no reflexion, for various values of γ. For $\gamma = \frac{5}{3}$, the ideal gas is compressed by a ratio of about 6·9.

9. The postulate of analyticity by Gelfand and Butler

The self-similar solution of the gasdynamic equations of the implosion problem was investigated by Gelfand who showed that there exists an interval of possible values of λ for the same γ. Gelfand then proposed to choose the particular single-valued self-similar coefficient λ, or $\alpha = 1/(1-\lambda)$, on the principle of analyticity of the resulting solution (Brushlinskii & Kazhdan 1963). Butler (1954) also investigated the implosion of an ideal gas with the aid of a high-speed computer and chose, from the various values of λ, the 'one non-singular' solution of the set of ordinary differential equations. We shall show now that this postulate of analyticity of Gelfand and Butler leads directly to the postulate of a single maximum in the pressure distribution, $d_\xi P = 0$, behind the shock front adopted in this paper.

With the aid of the transformation (2.8) we expressed the pressure and the density of the gas in terms of U; see (4.2). Equation (4.9) is the differential equation for U before any additional transformations. Its left-hand side is finite and at the singularity then, when the denominator of the right-hand side of equation (4.9) vanishes,

$$U\,d_\xi U + (1+\lambda)\,U + \lambda\xi = K[\gamma(\xi d_\xi U + U) + 2(\lambda+\gamma)\,\xi], \tag{9.1}$$

where K is an arbitrary number. Considering the conservation equations (2.12) the last differential equation reads

$$2\frac{\gamma-1}{(\gamma+1)^2}\frac{d_\xi P}{\mathscr{R}} = K\xi U\frac{d_\xi P}{P}, \tag{9.2}$$

or

$$\xi U\frac{d_\xi P}{P}\left[K - \frac{4}{\xi U\gamma(\gamma+1)^2}C^2\right] = 0, \tag{9.3}$$

where $C(\xi)$ is the reduced speed of sound, see (7.4). For an arbitrary K,

$$d_\xi P = 0; \tag{9.4}$$

see §4. When $K = (1/\gamma\xi)\,U$, with U the reduced speed at the singularity,

$$\frac{4}{(\gamma+1)^2}C^2 - U^2 = 0; \tag{9.5}$$

see (9.2) and §7, where it is shown that $-U = 2/(\gamma+1)C$ at the point where the pressure is maximum.

Equation (4.9) was obtained by an integration of the conservation equations (2.12), from the shock front at $\xi = 1$ to some arbitrary point ξ behind it. The left-hand side of (4.9) is finite and we considered the singularity on the right-hand side of this equation. Clearly other forms and equations could be investigated and analyticity studied differently. Butler, by postulating analyticity, arrives at a single-valued solution $\lambda(\gamma)$. In this paper a single-valued solution $\lambda(\gamma)$ is obtained by postulating a pressure maximum $d_\xi P = 0$, behind the shock front. It is clear then, in general, that the two postulates, of analyticity and of $d_\xi P = 0$, must concur, for there can be only one physically admissible solution $\lambda(\gamma)$ (Zeldovich & Raizer 1967, p. 801).

One of the authors (E.A.M.) is greatly indebted to Professor Paul S. Slosberg of Mount Sinai, New York.

Appendix

The discriminant of the quadratic equation (6.4)

$$[\lambda(2-\gamma)+\gamma]^2+4\gamma^2\lambda = 0, \tag{A 1}$$

when

$$\lambda = \frac{-\gamma}{(\gamma^{\frac{1}{2}}\pm 2^{\frac{1}{2}})^2}. \tag{A 2}$$

Insertion of the values of λ into the initial value $x(1)$ leads to

$$\frac{6\gamma(\gamma+1)}{(\gamma^{\frac{1}{2}}\pm 2^{\frac{1}{2}})^2}-(\gamma^2+6\gamma+1) < -(\gamma+1)^2 \tag{A 3}$$

(see (5.5)), or

$$\pm 4(2\gamma)^{\frac{1}{2}} > \gamma-1. \tag{A 4}$$

There can be no minus sign on the left-hand side of the last inequality for its right-hand side is positive, and the solution, $\lambda = -\lambda(\gamma^{\frac{1}{2}}-2^{\frac{1}{2}})^2$, is to be discarded.

The discriminant (A 1) is positive when

$$\lambda > \lambda_m = \frac{-\gamma}{(\gamma^{\frac{1}{2}}+2^{\frac{1}{2}})^2}. \tag{A 5}$$

It is easily seen that

$$\lambda = \lambda_0 = \frac{-\gamma(\gamma-1)}{(\gamma+1)(2\gamma-1)} \quad \text{for} \quad \gamma > 2+3^{\frac{1}{2}} \tag{A 6}$$

easily satisfies the (A 5) constraint.

REFERENCES

Butler, D. S. 1954 Converging spherical and cylindrical shocks. *Armament Res. Establishment, Theor. Res. Rep.* no. 54/54.

Brushlinskii, K. V. & Kazhdan, Ya. M. 1963 *Usp. Mat. Nauk* **3** (English trans. *Sov. Math. Surveys* **18**, 1).

Clark, J. S., Fisher, H. N. & Mason, R. J. 1973 *Phys. Rev. Lett.* **30**, 89.

Courant, R. & Friedrichs, K. U. 1957 *Sypersonic Flow and Shock Waves*. Interscience.

Fujimoto, Y. & Mishkin, E. A. 1977*a* Analysis of spherically imploding shocks. *Polytech. Inst. New York Tech. Rep.* PINY EE/EP 77-026.

Fujimoto, Y. & Mishkin, E. A. 1977*b* *11th Euro. Conf. Laser Interaction with Matter, Oxford Univ.*

Guderley, G. 1942 *Luftfahrtforschung* **19**, 302.

Kidder, R. E. 1974 *Nucl. Fusion* **14**, 53.

Landau, L. D. & Lifshitz, E. M. 1959 *Fluid Mechanics*. Addison-Wesley.

Lazarus, R. B. & Richtmyer, R. D. 1977 *Los Alamos Sci. Lab. Rep.* LA-6823. MS (June), p. 21.

Nuckolls, J., Wood, L., Thiessen, A. & Zimmerman, G. 1972 *Nature* **239**, 139.

Stanyukevich, K. P. 1960 *Unsteady Motion of Continuous Media*. Academic Press.

Taylor, G. I. 1946 *Proc. Roy. Soc.* A **186**, 273.

Zeldovich, Ya. B. & Raizer, Yu. P. 1967 *Physics of Shock Waves and High Temperature Hydrodynamic Phenomena*. Academic Press.